

UGAN: Untraceable GAN for Multi-Domain Face Translation

Defa Zhu¹, Si Liu², Wentao Jiang², Chen Gao¹, Tianyi Wu³, Qiangchang Wang⁴, Guodong Guo³

¹Chinese Academy of Sciences, ²Beihang University, ³Baidu Research, ⁴West Virginia University
 {zhudefa, gaochen}@iie.ac.cn, {liusi, jiangwentao}@buaa.edu.cn
 {wutianyi01, guogudong01}@baidu.com, qw0007@mix.wvu.edu

Abstract

The multi-domain image-to-image translation is a challenging task where the goal is to translate an image into multiple different domains. The target-only characteristics are desired for translated images, while the source-only characteristics should be erased. However, recent methods often suffer from retaining the characteristics of the source domain, which are incompatible with the target domain. To address this issue, we propose a method called Untraceable GAN, which has a novel source classifier to differentiate which domain an image is translated from, and determines whether the translated image still retains the characteristics of the source domain. Furthermore, we take the prototype of the target domain as the guidance for the translator to effectively synthesize the target-only characteristics. The translator is learned to synthesize the target-only characteristics and make the source domain untraceable for the discriminator, so that the source-only characteristics are erased. Finally, extensive experiments on three face editing tasks, including face aging, makeup, and expression editing, show that the proposed UGAN can produce superior results over the state-of-the-art models. The source code will be released.

1. Introduction

Multi-domain image-to-image translation [2] refers to image translation among multiple domains, where each domain is characterized by different attributes. For example, the face aging task, with age groups as domains, aims to translate a given face into other age groups using a single translator. As shown in Figure 1 Row 1, the input face image is translated into different age groups.

Although prior works [2, 33, 10] have made significant progress, the translated results still suffer from retaining the characteristics of the source domain (incompatible with the target domain), which is the so-called *phenomenon of source retaining*. As illustrated in Figure 1 Row 1, when StarGAN translates a female face from the age

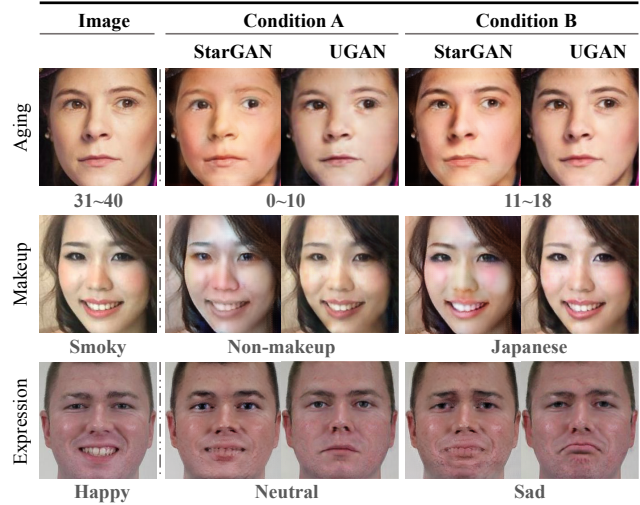


Figure 1. The phenomenon of source retaining in image translation. The first column shows input images. In the face aging case, when changing a face from 31 ~ 40 to 0 ~ 10, the result of StarGAN still looks like an adult while that of UGAN is more like a child with big eyes and smooth skin. When translating the face to 11 ~ 18, the result of UGAN also looks more like a juvenile. Similar observations can be made in expression and makeup editing tasks.

group 31~40 to 0~10, the translated image still looks like an adult. In makeup editing shown in Figure 1 Row 2, StarGAN fails to eliminate the eye shadows in makeup removing. For expression editing, as shown in Figure 1 Row 3, the results of StarGAN show visible teeth shadows around the mouth region.

The reason for *phenomenon of source retaining* is that the explicit and effective mechanisms to erase the characteristics of the source domain have not been explored in the prior works. Most of them just simply apply a domain classifier, which is only trained to recognize the domain class of real data, to guide the image translation. However, the domain classifier is not sensitive to the non-qualified synthesized image containing incompatible characteristics. As

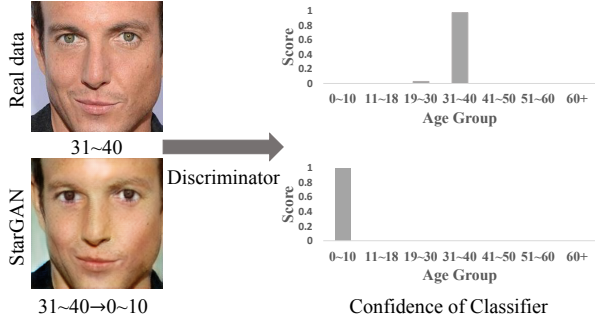


Figure 2. The domain classifier of the discriminator in StarGAN is easily deceived on face aging task. First row: Given an adult face within 31~40 age group from the test set, the domain classifier of the discriminator can successfully recognize the corresponding age. Second row: The adult face is translated into 0~10 years old, and the translated face heavily retains adult characteristics including beard and expression wrinkles. However, the classifier still doesn't identify the incompatible characteristics and is completely fooled by the translated face.

shown in Figure 2 Row 1, the discriminator correctly judges an adult face to be within 31~40 age group. Translating the adult face into a child face (0~10), the translated face heavily retains adult characteristics, e.g., beard and expression wrinkles (Figure 2 Row 2). However, the discriminator judges it to be within 0~10 age group with the confidence of 1. That is, the synthesized image containing incompatible characteristics has almost no punishment from the domain classifier, which results in the *phenomenon of source retaining*.

To tackle the problem of source retaining, we propose a new method untraceable GAN (UGAN), which introduces *untraceable constraint* and *prototype injection*. The untraceable constraint is employed to encourage the translator to erase all the source-only characteristics and synthesize certain target-only ones. As shown in Figure 2, the process of an image from 31~40 years old (source domain) translated to 0~10 years old (target domain), the beard and wrinkles (source-only characteristics) need to be erased, while a smooth skin and round face (target-only characteristics) should be synthesized. To endow the proposed UGAN with the above capabilities, a discriminator is trained to *track* which domain the synthesized image is *translated from*, while the translator is trained to make the source domain of the synthesized image being untraceable for the discriminator. Furthermore, To effectively synthesize the target-only characteristics, we take the prototype [13] of the target domain as the guidance for the translator. The prototype is a statistic of the target domain, which aims to provide the essential characteristics, like the round face of 0~10 years old domain.

Our contributions include:

- To the best of our knowledge, this is the first work to present the phenomenon of source retaining in multi-domain image-to-image translation, and propose a novel UGAN to explicitly erase the characteristics of the source domain for improving the image translation.
- A novel source classifier is introduced to differentiate which domain an image is translated from, and determines whether the translated image still retains the characteristics of the source domain.
- The propose UGAN is the first work to take the target prototype into the translator for synthesizing the target domain characteristics.
- Extensive qualitative and quantitative experiments are conducted for three face editing tasks that demonstrate the superiority of our proposed UGAN.

2. Related Work

In this section, we give a brief review on three aspects related to our work: Generative Adversarial Network, Conditional GANs and Image-to-Image Translation.

Generative Adversarial Networks (GANs) [7] are popular generative models that employ adversarial learning between a generator and discriminator to synthesize the realistic data, which have gained astonishing successes in many computer vision tasks, such as image-to-image translation [12], domain adaptation [19] and super-resolution [15]. In this work, the proposed UGAN enjoys the adversarial learning [1, 8], which approximately minimizes the Wasserstein distance between the synthesized distribution and real distribution.

Conditional GANs [20] are variants of GANs, which aim to controllably synthesize examples under the given condition. Many prior works focus on generating samples under different forms of conditions, such as category label in the form of one-hot code [20] or learnable parameters [21], and text with word embedding [31], etc. Different from these works, for synthesizing the required characteristics, we introduce the prototype of the condition to provide prior information, where the prototype is one of the statistics of the target domain.

Image-to-Image Translation is first defined in pix2pix [12], which is improved from various aspects, such as skip connection for maintaining useful original information [30, 18, 24], cascade training from coarse to fine [27, 3], extra relevant data [2], buffer of history fake image [25], multi-discriminator [27], 3D technology [29], variational sampling [35, 6]. If the translator only models directed translation between two domains, $C \cdot (C - 1)$ translators are required among C domains. A single conditional translator for multi-domain translation is seriously demanded. Thus we focus on multi-domain translation

with such a single translator. The current multi-domain image translation methods [2, 33, 10] using the vanilla one-hot condition for the translator, without considering the information contained in each domain. We are the first to adopt the statistics of each domain as a condition of the translator to efficiently inject the essential characteristics. Furthermore, the prior methods apply the domain classifier for condition constraints. However, limited by the classifier, they often suffer from the *phenomenon of source retaining*. Thus, we change the role of this auxiliary classifier in UGAN and make it classify which source domain the given datum is translated from, instead of classifying which domain the given datum is sampled from.

3. Our Approach

The framework of UGAN is shown in Figure 3. The input image and the target condition are fed into the translator G . The discriminator D has two heads: one head is named as the authenticity classifier to distinguish whether the input sample is real or fake; the other is called the source classifier, aiming to determine which domain the sample is translated from, where the real data are supposed to be translated from themselves. For erasing source-only characteristics and synthesizing the target-only characteristics, translator G is trained to fool the source classifier of D to believe that the synthesized image is translated from the target domain. Moreover, to effectively synthesize the target characteristics, we introduce the “prototype” of the target domain and inject it into the translated image.

For convenience, we then introduce the used mathematical annotations. Discriminator D here contains two heads including the authenticity classifier D_a and the source classifier D_s , where D_a and D_s share the same feature extraction module D_f . $D_a(D_f(\cdot))$ and $D_s(D_f(\cdot))$ are abbreviated as $D_a(\cdot)$ and $D_s(\cdot)$ respectively. $\{x_s, y_s\}$ is a sample pair from the source domain, where x_s represents the image and y_s is its label. By feeding the image x_s and the target label y_t into G , it produces $\tilde{x}_{s \rightarrow t} = G(x_s, y_t)$. We use $q(x, y)$ to denote the joint distribution of image x and domain label y . $q(x)$ and $q(y)$ are the marginal distribution of images and labels, respectively.

3.1. Untraceable Constraint

To tackle the problem of source retaining, the source classifier D_s is trained to classify which domain image x is translated from. For an real image-label pair $\{x_s, y_s\}$, we regard x_s as translated from domain y_s to domain y_s . Since D_s aims to classify where an image is translated from, the real datum x_s should be classified into y_s , meaning x_s is translated from domain y_s . The synthesized image $\tilde{x}_{s \rightarrow t}$ should be classified into y_s , meaning $\tilde{x}_{s \rightarrow t}$ is translated from y_s . Translator G is trained to fool D_s to classify $\tilde{x}_{s \rightarrow t}$ into the y_t . In this way, G is trained to make the source

domain of $\tilde{x}_{s \rightarrow t}$ is untraceable and the target domain characteristics are injected to $\tilde{x}_{s \rightarrow t}$. The adversarial training is formulated as follows:

$$L_D^{S_1} = -E_{(x_s, y_s)}[\log D_s(x_s, y_s)] - \lambda_u E_{(x_s, y_s), y_t}[\log D_s(G(x_s, y_t), y_s)], \quad (1)$$

$$L_G^{S_1} = -\lambda_u E_{(x_s, y_s), y_t}[\log D_s(G(x_s, y_t), y_t)], \quad (2)$$

where λ_u is the penalty coefficient of source retaining. For space limit, $E_{(x, y) \sim q(x, y)}[\cdot]$ and $E_{y \sim q(y)}[\cdot]$ are abbreviated as $E_{(x, y)}[\cdot]$ and $E_y[\cdot]$, respectively.

Note that the $\tilde{x}_{s \rightarrow t}$ should be injected with certain target-only characteristics. Recall that in Eq. (2), G is trained to fool D_s to classify $\tilde{x}_{s \rightarrow t}$ into y_t . However, the class y_t here is not pure that mixed with the characteristics of x_t and synthesized data $\tilde{x}_{t \rightarrow ?}$. Refer to Eq. (1), the source classifier D_s treats the real sample x_t sampled from y_t and fake sample $\tilde{x}_{t \rightarrow ?}$ translated from y_t as the same class y_t . To accurately synthesize the characteristics of the target domain, the number of categories of D_s is augmented as $2C$. The first C categories are real data and those sampled (translated) from the corresponding domain. The latter C categories are fake data, and those translated from the corresponding domain. $y_s + C$ means input datum is fake and translated from y_s . In addition, the translator G is trained to fool D_s to classify $\tilde{x}_{s \rightarrow t}$ into the y_t category. The untraceable constraint conducted via optimizing the following:

$$L_D^{S_2} = -E_{(x_s, y_s)}[\log D_s(x_s, y_s)] - \lambda_u E_{(x_s, y_s), y_t}[\log D_s(G(x_s, y_t), y_s + C)], \quad (3)$$

$$L_G^{S_2} = -\lambda_u E_{(x_s, y_s), y_t}[\log D_s(G(x_s, y_t), y_t)]. \quad (4)$$

In this process, D_s is trained to identify whether $\tilde{x}_{s \rightarrow t}$ is a fake image and the source domain. G is trained to approximate the true untraceable translator.

3.2. Prototype Injection

The statistics of the target domain can provide guidance information for image translation. Refer to Figure 3 (b), the average image of each age group shows the essential characteristics, like round face and flat nose characteristics of age group 1 (0~10). Thus, We leverage the statistics of the target domain to further inject the essential characteristics of the target domain into the translated image, where we call the statistic, containing the essential characteristics, as the “prototypes” following the classic aging method [13]. However, the posture of the source image and target prototype may be misaligned. Thus, concatenating or summing up the image feature and prototype feature will hurt the performance. To naturally inject these essential characteristics, we design an adaptive prototype injection (API) module inspired by non-local operation [28, 26].

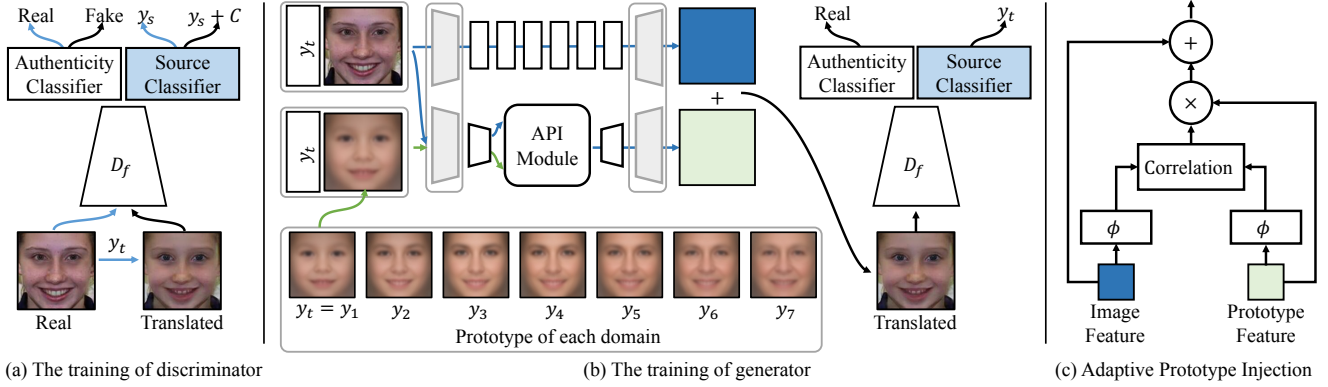


Figure 3. An overview of UGAN. a) The discriminator D should not only distinguish whether the input sample is real or fake but also determine which domain the sample is translated from. b) Translator G is trained to fool D by synthesizing realistic images of the target domain. We take the average image as a ‘‘prototype’’ to inject prior information of the target domain. c) The adaptive prototype injection is introduced for injecting essential characteristics of the prototype into the source image.

Refer to Figure 3 (c), the injection process of API is formulated as follows:

$$\begin{aligned} \mathcal{A}_{ij} &= \frac{\exp(\phi(f_i^x) \cdot \phi(f_j^p))}{\sum_{\forall k} \exp(\phi(f_i^x) \cdot \phi(f_k^p))}, \\ f_i^{\text{inject}} &= f_i^x + \sum_{\forall j} \mathcal{A}_{ij} \cdot f_j^p, \end{aligned} \quad (5)$$

where f^x and f^p are the feature maps of the source image and target prototype, respectively. i is the index of a feature map position. ϕ is a linear mapping to reduce the dimension. Since the computation of the correlation matrix \mathcal{A} is computationally expensive, we apply the API module on the low-resolution feature maps. To simultaneously maintain resolution and inject the prototype, the translator G is designed with two parallel networks, with parameter sharing at both ends (gray color, Figure 3). For maintaining the resolution, one network is a common architecture in image translation [34]. The other one applies the API module on the low-resolution feature maps. Finally, the outputs of these two networks are fused by element-wise sum to generate the translated image.

3.3. Objective Function

Authenticity constraint: The adversarial loss of WGAN-gp [8] is adopted to constrain the synthetic joint distribution to approximate the real distribution.

$$L_D^A = -E_{x_s} [D_a(x_s)] + E_{x_s, y_t} [D_a(G(x_s, y_t))] + \lambda_{gp} E_{\hat{x}} [(\|\nabla_{\hat{x}} [D_a(\hat{x})]\|_2 - 1)^2], \quad (6)$$

$$L_G^A = -E_{x_s, y_t} [D_a(G(x_s, y_t))], \quad (7)$$

where $\hat{x} = \alpha \cdot x_s + (1 - \alpha) \cdot G(x_s, y_t)$, and $\alpha \sim U(0, 1)$. The third term in Eq. (6) is a gradient penalty term that enforces the discriminator as a 1-Lipschitz function.

Cycle Consistency: The input and output are regularized to satisfy the correspondence [34]:

$$L_G^C = \lambda_c E_{(x_s, y_s), y_t} [\|G(G(x_s, y_t), y_s) - x_s\|_1] \cdot S \quad (8)$$

Overall loss function: D and G are trained by optimizing

$$L_D^U = L_D^A + L_D^S, \quad (9)$$

$$L_G^U = L_G^C + L_G^A + L_G^S, \quad (10)$$

where L^S could be L^{S1} or L^{S2} . The Eq. (9) and Eq. (10) are optimized alternatively.

4. Experiments

4.1. Datasets

Face aging dataset is collected by C-GAN [18] including 15,030 face images. Ages are divided into 7 age groups including 0 ~ 10, 11 ~ 18, 19 ~ 30, 31 ~ 40, 41 ~ 50, 51 ~ 60 and 60+. 10% of the dataset is randomly selected as the test set, and the rest is the training set.

MAKEUP-A5 is a makeup-labeled dataset [17] containing 6,095 aligned Asian woman faces with 5 makeup categories including retro, Korean, Japanese, non-makeup and smoky. The training set contains 5,485 images and the remaining is the test set.

CFEE is an expression dataset [5] of 22 expressions with 5,060 images. The categories of facial expressions include (A) neutral, (B) happy, (C) sad, (D) fearful, (E) angry, (F) surprised, (G) disgusted, (H) happily surprised, (I) happily disgusted, (J) sadly fearful, (K) sadly angry, (L) sadly surprised, (M) sadly disgusted, (N) fearfully angry, (O) fearfully surprised, (P) fearfully disgusted, (Q) angrily surprised, (R) angrily disgusted, (S) disgustedly surprised, (T) appalled, (U) hatred and (V) awed. We randomly select

Table 1. Intra FID on CFEE dataset.

Method	A	B	C	D	E	F	G	H	I	J	K	L	M	N	O	P	Q	R	S	T	U	V	Mean
StarGAN	52.1	52.6	61.4	51.5	55.9	64.1	57.8	54.1	42.6	52.5	61.7	69.3	55.2	51.9	55.0	63.2	68.0	60.6	69.9	61.0	59.1	61.3	58.2
UGAN [†]	44.5	44.4	53.8	46.9	49.9	59.0	47.8	48.5	37.7	43.2	52.9	59.1	53.4	50.4	53.0	45.6	56.6	52.7	48.4	49.0	47.0	46.4	49.6
UGAN [‡]	42.8	45.3	48.3	43.7	47.5	56.0	43.6	44.7	37.6	41.4	47.4	52.4	42.9	43.1	48.5	46.3	52.1	46.6	46.6	46.8	45.4	45.0	46.1
UGAN	39.7	40.8	47.9	39.7	43.8	57.6	42.0	43.1	33.5	40.8	45.7	55.4	40.8	40.9	46.9	43.4	52.3	47.3	44.9	48.1	42.0	48.5	44.8

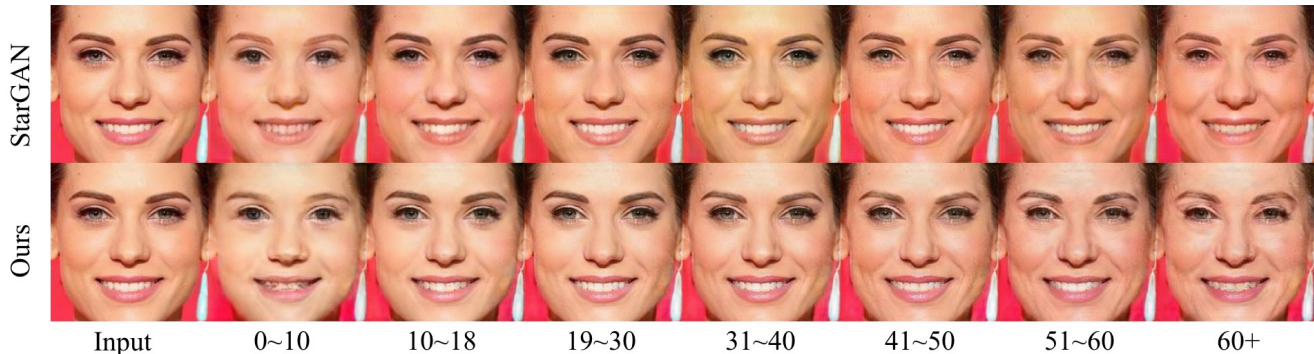


Figure 4. Comparison of face aging synthesis results on the face aging dataset.

Table 2. Intra FID on face aging dataset.

method	0~10	11~18	19~30	31~40	41~50	51~60	60+	Mean
CAAE	63.8	64.1	67.6	69.8	75.9	78.7	87.2	72.4
C-GAN	83.9	60.7	54.9	54.7	57.4	61.7	70.2	63.4
StarGAN	59.9	38.2	29.9	41.4	37.3	40.0	46.9	41.9
UGAN [†]	42.0	33.6	25.2	27.2	28.9	34.4	40.4	33.1
UGAN [‡]	44.0	29.5	21.1	21.3	25.4	28.2	34.7	29.2
UGAN	42.7	28.4	19.4	18.9	22.8	26.9	32.5	27.4

Table 3. Intra FID on MAKEUP-A5 dataset.

method	Retro	Korean	Japanese	Non-makeup	Smoky	Mean
StarGAN	110.9	86.2	74.5	84.4	91.9	89.6
UGAN [†]	109.4	70.9	61.8	72.8	74.8	78.0
UGAN [‡]	101.7	65.9	58.1	64.5	66.3	71.3
UGAN	89.6	73.3	57.1	62.1	68.8	70.2

23 identities (506 images) as the test set and use the other images for training. All images are aligned and resized to 256×256 resolution.

4.2. Measurements

Intra FIDs [11, 22, 4] on each domain and mean of them are used for evaluation. FID is a common quantitative measure for generative models, which measures the 2-Wasserstein distance between the two distributions q and p on the features extracted from InceptionV3 model. It is

defined as [4]

$$F(q, p) = \|\mu_q - \mu_p\|_2^2 + \text{tr}(\sigma_q + \sigma_p - 2(\sigma_q \sigma_p)^{1/2}), \quad (11)$$

where q and p are feature distributions of real data and synthesized data, (μ_q, σ_q) and (μ_p, σ_p) are the mean and the covariance of q and p . The mean intra FID is calculated by

$$mF_{intra}(q, p) = \frac{1}{C} \sum_{i=1}^C F(q(\cdot|y_i), p(\cdot|y_i)), \quad (12)$$

where y is the domain label for the total C domains.

User studies by Amazon Mechanical Turk (AMT): Given an input image, target domain images translated by different methods are displayed to the Turkers who are asked to choose the best one.

Cosine similarity: For the face aging task, cosine similarity between the features of real images and the corresponding translated images is used to measure the degree of source retaining. Features are extracted by a ResNet-18 model [9] trained on the same training set.

4.3. Implementation Details

We perform experiments with three versions of our methods named as UGAN[†], UGAN[‡] and UGAN, where the methods with superscripts ([†] and [‡]) mean adopting the same translator as StarGAN (without prototype), “UGAN[†]” means adopting L^{S1} as untraceable constraint, while “UGAN[‡]” adopting L^{S2} . “UGAN” means the final method that adopting L^{S2} as an untraceable constraint and the proposed translator with an API module. For a fair comparison, our learning rate is fixed as 0.0001, while the

Table 4. AMT results on CFEE dataset(%).

Method	A	B	C	D	E	F	G	H	I	J	K	L	M	N	O	P	Q	R	S	T	U	V
StarGAN	17.0	8.7	13.7	14.7	29.0	13.7	33.3	14.7	22.0	19.0	18.7	22.7	31.3	29.0	17.0	13.3	18.3	27.0	37.7	19.0	19.3	7.3
UGAN	83.0	91.3	86.3	85.3	71.0	86.3	66.7	85.3	78.0	81.0	81.3	77.3	68.7	71.0	83.0	86.7	81.7	73.0	62.3	81.0	80.7	92.7

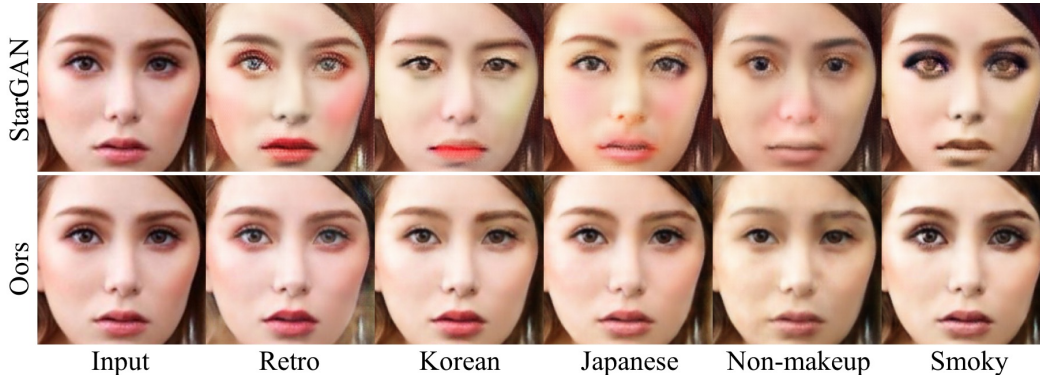


Figure 5. Makeup synthesis results on the MAKEUP-A5.

Table 5. AMT results on face aging dataset (%).

Method	0~10	11~18	19~30	31~40	41~50	51~60	60+
StarGAN	13.0	34.3	34.3	42.3	39.7	10.7	13.0
UGAN	87.0	65.7	65.7	57.7	60.3	89.3	87.0

Table 6. AMT results on MAKEUP-A5 dataset (%).

Method	Retro	Korean	Japanese	Non-makeup	Smoky
StarGAN	28.7	40.3	21.3	16.7	30.7
UGAN	71.3	59.7	78.7	83.3	69.3

Table 7. Cosine similarity on hidden feature of ResNet-18 between source images and the corresponding translated images.

Method	Age Group Gap			
	≥ 3	≥ 4	≥ 5	≥ 6
StarGAN	0.757	0.742	0.745	0.719
UGAN	0.740	0.714	0.712	0.696

other hyper-parameters are kept the same as StarGAN. All experiments are optimized by Adam with $\beta_1 = 0.5$ and $\beta_2 = 0.999$. The discriminator is iterated 5 times per iteration of the translator. All baselines and our methods are trained 200 epochs. The mini-batch size is set to 16. All images are horizontally flipped with a probability of 0.5 as data augmentation.

Baselines: StarGAN [2] has shown the best performance than DIAT [16], CycleGAN [34] and IcGAN [23]. We, therefore, select StarGAN as our baseline to verify the superiority of our method. For the face aging task, we additionally compare two classic GAN-based methods of face

aging, including CAEE [32] and C-GAN (without transition pattern network) [18].

4.4. Quantitative Experiments

Given the domain label y_i , we traverse all images in the test set to generate fake images. All the synthetic images of each domain are adopted to calculate intra FID, while 300 synthetic images of each domain are randomly sampled to be evaluated by AMT.

Face aging: The comparison of results on face aging dataset is shown in Table 2. Face aging involves deformations and texture synthesis. For example, deformation, such as the face shape and eye size, are the main differences between babies and adults. Texture synthesis, like adding wrinkles, is also essential when translating a middle-aged man to a senior man. In Table 2, both UGAN[†] and UGAN[‡] are significantly better than StarGAN on all age groups, where UGAN[‡] are better than UGAN[†]. The mean intra FID drops from 41.9 (StarGAN) to 29.2 (UGAN[‡]). The relative drop is more than 30%. Furthermore, UGAN achieves the best performance with mean intra FID 27.4.

Makeup editing: The comparison of results on MAKEUP-A5 dataset is shown in Table 3. Both texture and color need to be altered in makeup editing. UGAN has the best performance in all categories. The mean intra FID has declined from 89.6 (StarGAN) to 71.3 (UGAN).

Expression editing: The comparisons on CFEE dataset are shown in Table 1. The expression editing task aims to change the emotion of a face by deformation. The CFEE dataset contains 22 kinds of fine-grained expressions, which makes the expression editing problem very challenging. From the results, we can conclude that UGAN again



Figure 6. Comparison of facial expression editing results on the CFEE dataset.

achieves the best performance. The mean intra FID is 58.2 (StarGAN), 49.6 (UGAN[†]), 46.1 (UGAN[‡]), and 44.8 (UGAN), respectively. It can be seen that the reduction is significant.

AMT user studies: For further evaluation, user studies are conducted on AMT¹ to compare StarGAN and our method. Since UGAN outperforms UGAN[†] and UGAN[‡] for mean intra FID, only UGAN is compared. With datasets mentioned above, we synthesize 300 pairs of images per domain by UGAN and StarGAN. All image pairs are shown to 102 Turkers who are asked to choose the better one considering image realism and satisfaction of target characteristics. Table 4, 5 and 6 show the percentage of our method beating StarGAN. For example, in Table 5, when changing

¹<https://www.mturk.com/>

a face to 0 ~ 10 years old, StarGAN wins in 13.2% cases while our method wins in 86.8% cases. It again shows the advantages of our method when transforming a face into childhood. Generally, our method is better than StarGAN in every category of each dataset.

Tackling the phenomenon of source retaining: The effect of erasing source characteristics on face aging is shown in Table 7. A well-trained ResNet-18 (for age recognition) is adopted to extract features (the second last layer). We calculate average cosine similarity on the neural feature of all source images and translated image pairs from the test set. Intuitively, the smaller the similarity, the more thoroughly source characteristics are erased. Since the images of adjacent age groups are similar, we only consider translation across a large age gap, e.g., across three age groups. In Table 7, we perform the experiments on multiple age group

gaps, and the similarities of UGAN are smaller on all age group gaps.

4.5. Qualitative Experiments

The visualization results are shown in Figure 4, 5 and 6. More results are provided in supplementary material.

Face aging: Results on the face aging dataset are shown in Figure 4. In the first example, an input image is a woman. By comparing the results of 0 ~ 10 years old (second column), our result has obvious childish characteristics, *e.g.* round face, big eyes, and small nose, while the result of StarGAN does not look like a child. Another example is the 60+ years old case (last column). Our result has white hair, wrinkles, while StarGAN produces a middle-aged face. These results show that UGAN can explicitly erase the characteristics of the source image by the source classifier in the discriminator.

Makeup editing: Two exemplary results on MAKEUP-A5 dataset are displayed in Figure 5. For the first woman, by comparing the results of the second (retro) and last (smoky) columns, we find that blusher and eye shadows of UGAN are more natural, while StarGAN draws asymmetrical blusher and strange eye shadows. The result of UGAN is relatively natural when translating it to a non-makeup face. Therefore, we conclude that UGAN has learned the precise color and texture characteristics of different makeups.

Expression editing: Results on CFEE dataset are demonstrated in Figure 6. We have the following observations. First, UGAN can well edit 22 kinds of fine-grained facial expressions. Also, UGAN captures the subtle differences between basic and compound expressions. For example, “Happily surprised” has bigger eyes and raising eyebrows compared to “Happy”. Besides, the results of StarGAN under various expressions still retain the original expressions. For example, when changing the man from “Hatred” to “Happy”, the result of StarGAN still has tight brows. Comparatively, UGAN can effectively synthesize the “Happy” expression by generating a grin and relaxed brows and erasing the tight brows.

5. Conclusion

The phenomenon of source retaining often occurs in the image-to-image translation task. To address it, the Untraceable GAN (UGAN) model has been proposed, where the discriminator estimates the source domain. The translator G is trained to fool the discriminator D to believe that the generated data is translated from the target domain. In this way, the source domain of the synthesized image is untraceable. In addition, we have further presented the prototype of each domain and inject it into the translated image to generate the target characteristics. Extensive experiments on three tasks have proven the significant advantages of our method over the state-of-the-art StarGAN.

The source retaining phenomenon is common in various fields, where the UGAN idea may be widely used to alleviate the issue. For example, language translation [14] often preserves the grammatical structure of the source language. UGAN may serve as a solution to improve translation quality. Furthermore, the prototype injection idea also can be introduced to the universal conditional generation. We plan to study these ideas in-depth and apply them to broader applications.

References

- [1] M. Arjovsky, S. Chintala, and L. Bottou. Wasserstein gan. *arXiv:1701.07875*, 2017.
- [2] Y. Choi, M. Choi, M. Kim, J.-W. Ha, S. Kim, and J. Choo. Stargan: Unified generative adversarial networks for multi-domain image-to-image translation. In *CVPR*, 2018.
- [3] T. Dekel, C. Gan, D. Krishnan, C. Liu, and W. T. Freeman. Sparse, smart contours to represent and edit images. In *CVPR*, 2018.
- [4] D. Dowson and B. Landau. The fréchet distance between multivariate normal distributions. *MA*, 1982.
- [5] S. Du, Y. Tao, and A. M. Martinez. Compound facial expressions of emotion. *PNAS*, 2014.
- [6] P. Esser, E. Sutter, and B. Ommer. A variational u-net for conditional appearance and shape generation. In *CVPR*, 2018.
- [7] I. J. Goodfellow, J. Pougetabadi, M. Mirza, B. Xu, D. Wardefarley, S. Ozair, A. Courville, and Y. Bengio. Generative adversarial networks. In *NIPS*, 2014.
- [8] I. Gulrajani, F. Ahmed, M. Arjovsky, V. Dumoulin, and A. C. Courville. Improved training of wasserstein gans. In *NIPS*, 2017.
- [9] K. He, X. Zhang, S. Ren, and J. Sun. Deep residual learning for image recognition. In *CVPR*, 2016.
- [10] Z. He, W. Zuo, M. Kan, S. Shan, and X. Chen. Attgan: Facial attribute editing by only changing what you want. *IEEE Transactions on Image Processing*, 2019.
- [11] M. Heusel, H. Ramsauer, T. Unterthiner, B. Nessler, and S. Hochreiter. Gans trained by a two time-scale update rule converge to a local nash equilibrium. In *NIPS*, 2017.
- [12] P. Isola, J.-Y. Zhu, T. Zhou, and A. A. Efros. Image-to-image translation with conditional adversarial networks. In *CVPR*. IEEE, 2017.
- [13] I. Kemelmacher-Shlizerman, S. Suwajanakorn, and S. M. Seitz. Illumination-aware age progression. In *CVPR*, 2014.
- [14] G. Lample, A. Conneau, L. Denoyer, and M. Ranzato. Un-supervised machine translation using monolingual corpora only. *ICLR*, 2018.
- [15] C. Ledig, L. Theis, F. Huszár, J. Caballero, A. Cunningham, A. Acosta, A. P. Aitken, A. Tejani, J. Totz, Z. Wang, et al. Photo-realistic single image super-resolution using a generative adversarial network. In *CVPR*, 2017.
- [16] M. Li, W. Zuo, and D. Zhang. Deep identity-aware transfer of facial attributes. *arXiv:1610.05586*, 2016.

- [17] T. Li, R. Qian, C. Dong, S. Liu, Q. Yan, W. Zhu, and L. Lin. Beautygan: Instance-level facial makeup transfer with deep generative adversarial network. In *MM*, 2018.
- [18] S. Liu, Y. Sun, D. Zhu, R. Bao, W. Wang, X. Shu, and S. Yan. Face aging with contextual generative adversarial nets. In *MM*, 2017.
- [19] S. Liu, Y. Sun, D. Zhu, G. Ren, Y. Chen, J. Feng, and J. Han. Cross-domain human parsing via adversarial feature and label adaptation. *arXiv:1801.01260*, 2018.
- [20] M. Mirza and S. Osindero. Conditional generative adversarial nets. *arXiv:1411.1784*, 2014.
- [21] T. Miyato, T. Kataoka, M. Koyama, and Y. Yoshida. Spectral normalization for generative adversarial networks. *arXiv:1802.05957*, 2018.
- [22] T. Miyato and M. Koyama. cgans with projection discriminator. *arXiv:1802.05637*, 2018.
- [23] G. Perarnau, J. van de Weijer, B. Raducanu, and J. M. Álvarez. Invertible conditional gans for image editing. *arXiv:1611.06355*, 2016.
- [24] A. Pumarola, A. Agudo, A. M. Martinez, A. Sanfeliu, and F. Moreno-Noguer. Ganimation: Anatomically-aware facial animation from a single image. In *ECCV*, 2018.
- [25] A. Shrivastava, T. Pfister, O. Tuzel, J. Susskind, W. Wang, and R. Webb. Learning from simulated and unsupervised images through adversarial training. In *CVPR*, 2017.
- [26] A. Vaswani, N. Shazeer, N. Parmar, J. Uszkoreit, L. Jones, A. N. Gomez, Ł. Kaiser, and I. Polosukhin. Attention is all you need. In *NIPS*, 2017.
- [27] T.-C. Wang, M.-Y. Liu, J.-Y. Zhu, A. Tao, J. Kautz, and B. Catanzaro. High-resolution image synthesis and semantic manipulation with conditional gans. *arXiv:1711.11585*, 2017.
- [28] X. Wang, R. Girshick, A. Gupta, and K. He. Non-local neural networks. In *CVPR*, 2018.
- [29] S. Yao, T. M. H. Hsu, J.-Y. Zhu, J. Wu, A. Torralba, B. Freeman, and J. Tenenbaum. 3d-aware scene manipulation via inverse graphics. *arXiv:1808.09351*, 2018.
- [30] G. Zhang, M. Kan, S. Shan, and X. Chen. Generative adversarial network with spatial attention for face attribute editing. In *ECCV*, 2018.
- [31] H. Zhang, T. Xu, H. Li, S. Zhang, X. Huang, X. Wang, and D. Metaxas. Stackgan: Text to photo-realistic image synthesis with stacked generative adversarial networks. *arXiv preprint*, 2017.
- [32] Z. Zhang, Y. Song, and H. Qi. Age progression/regression by conditional adversarial autoencoder. In *CVPR*, 2017.
- [33] B. Zhao, B. Chang, Z. Jie, and L. Sigal. Modular generative adversarial networks. In *ECCV*, 2018.
- [34] J.-Y. Zhu, T. Park, P. Isola, and A. A. Efros. Unpaired image-to-image translation using cycle-consistent adversarial networks. *arXiv:1703.10593*, 2017.
- [35] J.-Y. Zhu, R. Zhang, D. Pathak, T. Darrell, A. A. Efros, O. Wang, and E. Shechtman. Toward multimodal image-to-image translation. In *NIPS*, 2017.

Appendices

A. Network Architecture

The architectures of the generator and discriminator are shown in Figure. 7 and 8.

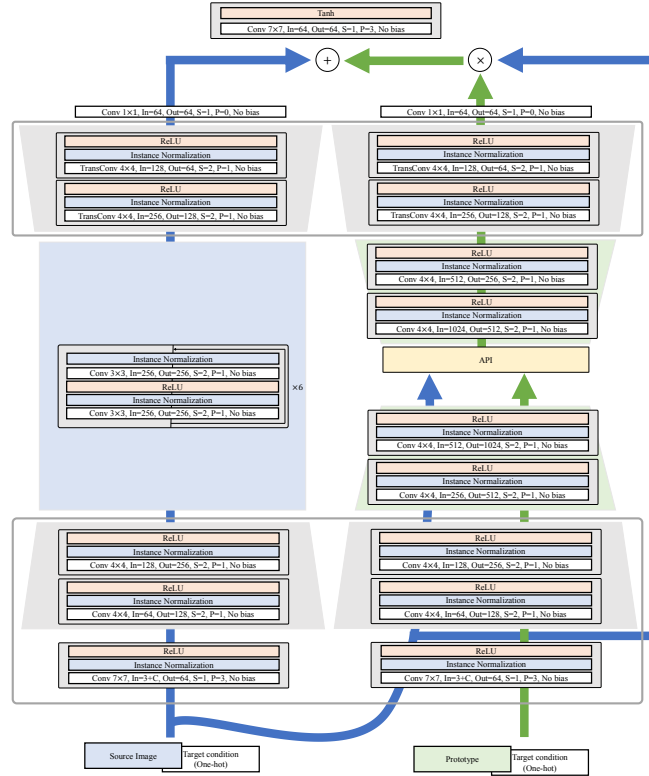


Figure 7. The architecture of the generator.

B. Prototype

We take the average image of as the prototype of each domain. The average images of the datasets are shown in Figure 9, 10, 11.

C. Qualitative Results

The face editing results on face aging, MAKEUP-A5 (makeup editing) and CFEE (expression editing) datasets are shown in Figure 12, 13, 14, 15, 16 and 17.

Face aging: the results on face aging dataset are shown in Figure 12 and 13. In the Figure 12, the women images are used as input and synthesized faces of seven age groups are shown in second to seventh columns. Observing the second and last columns, our method generates very realistic results. For example, in the sixth row and fourth column (*row 6, col 4*) of Figure 12, the woman is successfully transformed into a child with baby teeth, big eyes, etc. For another example, in (*row 4, col 8*) the woman is aged to a senior woman with white hair and wrinkles. Similar conclusions can be drawn by taking men as input as shown in 13. For example, in (*row 2, col 4 ~ 6*), the beard of the translated images become increasingly thicker.

Makeup editing: 4 exemplar results of StarGAN and UGAN on MAKEUP-A5 are displayed in Figure 14 and 15 respectively. Observing the images of the fifth column, all makeup can be removed to be a naked face. By observing the others columns, the makeup results of our method correspond to the specified categories. For example, in (*row 8, col 2*) of Figure 14, the translated face belongs to “Retro” with pink blush, lipstick, eye shadow. For another example, in (*row 8, col 6*) of Figure 14, the translated face belongs to “Smoky” with black eyeliner and eye shadow.

Expression editing: 2 exemplar results of expression editing on CFEE are demonstrated in Figure 16 and 17 respectively. Our method is able to edit 22 kinds of fine-grained facial expression well. For example, for the image in the second row of Figure 17, when translating it

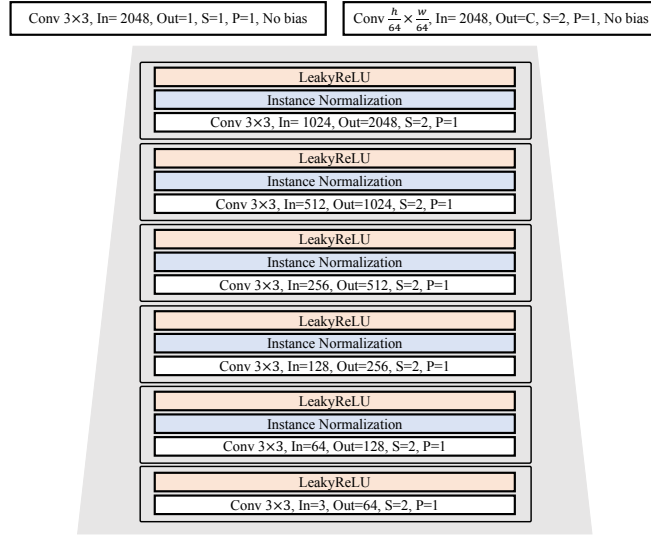


Figure 8. The architecture of the discriminator.



Figure 9. Average images of face aging dataset.



Figure 10. Average images of MAKEUP-A5 dataset.

to “happy”, our method successfully synthesizes the real teeth and accurately expresses the happy expression. Our method also can vividly synthesize other expressions.

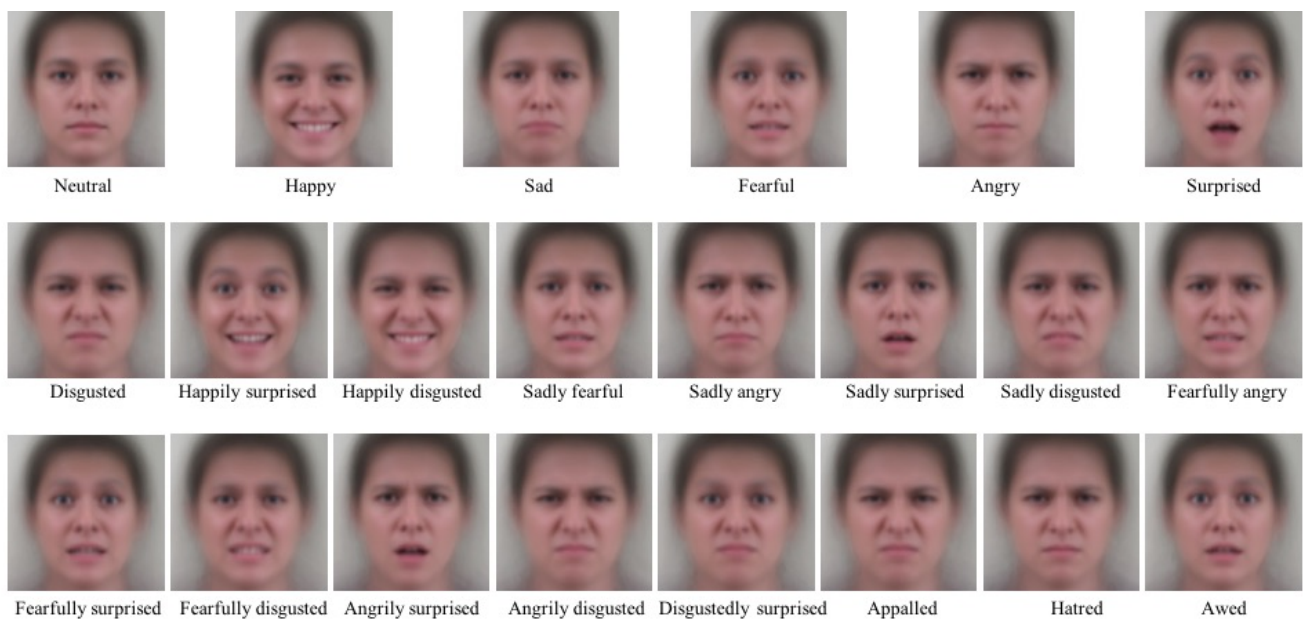


Figure 11. Average images of CFEE dataset.



Figure 12. Face aging results on the face aging dataset.

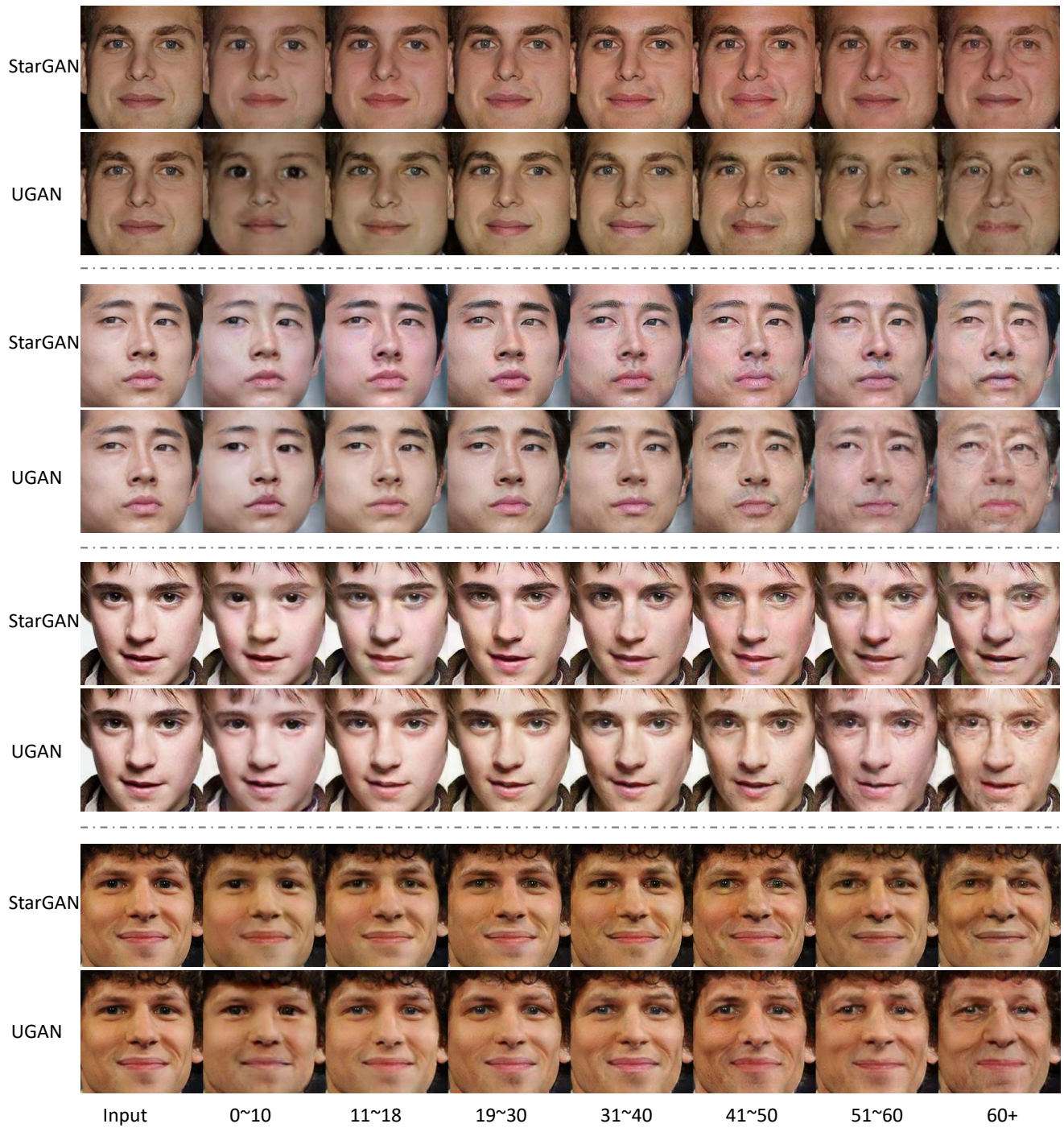


Figure 13. Face aging results on the face aging dataset.

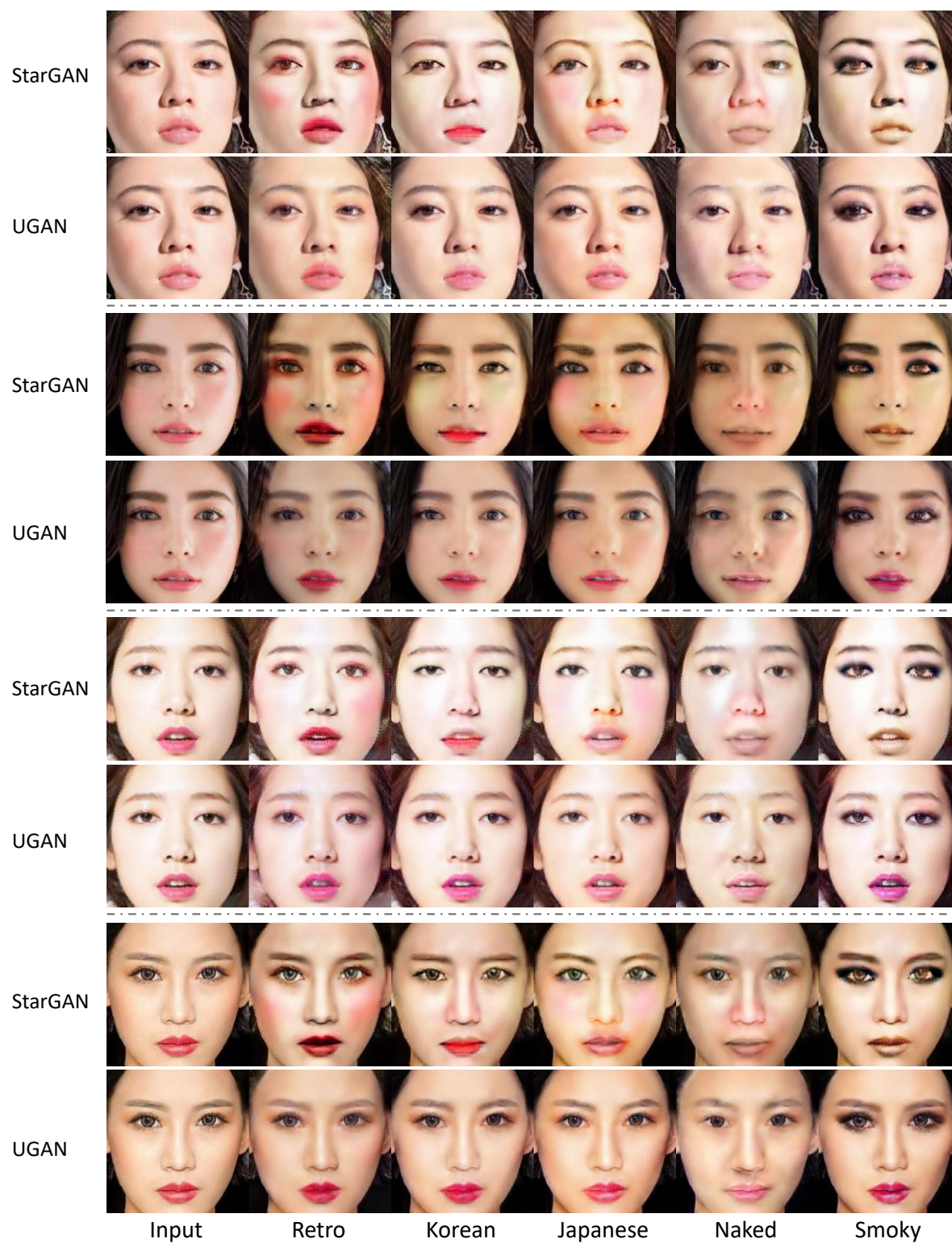


Figure 14. Makeup editing results on the MAKEUP-A5 dataset.



Figure 15. Makeup editing results on the MAKEUP-A5 dataset.

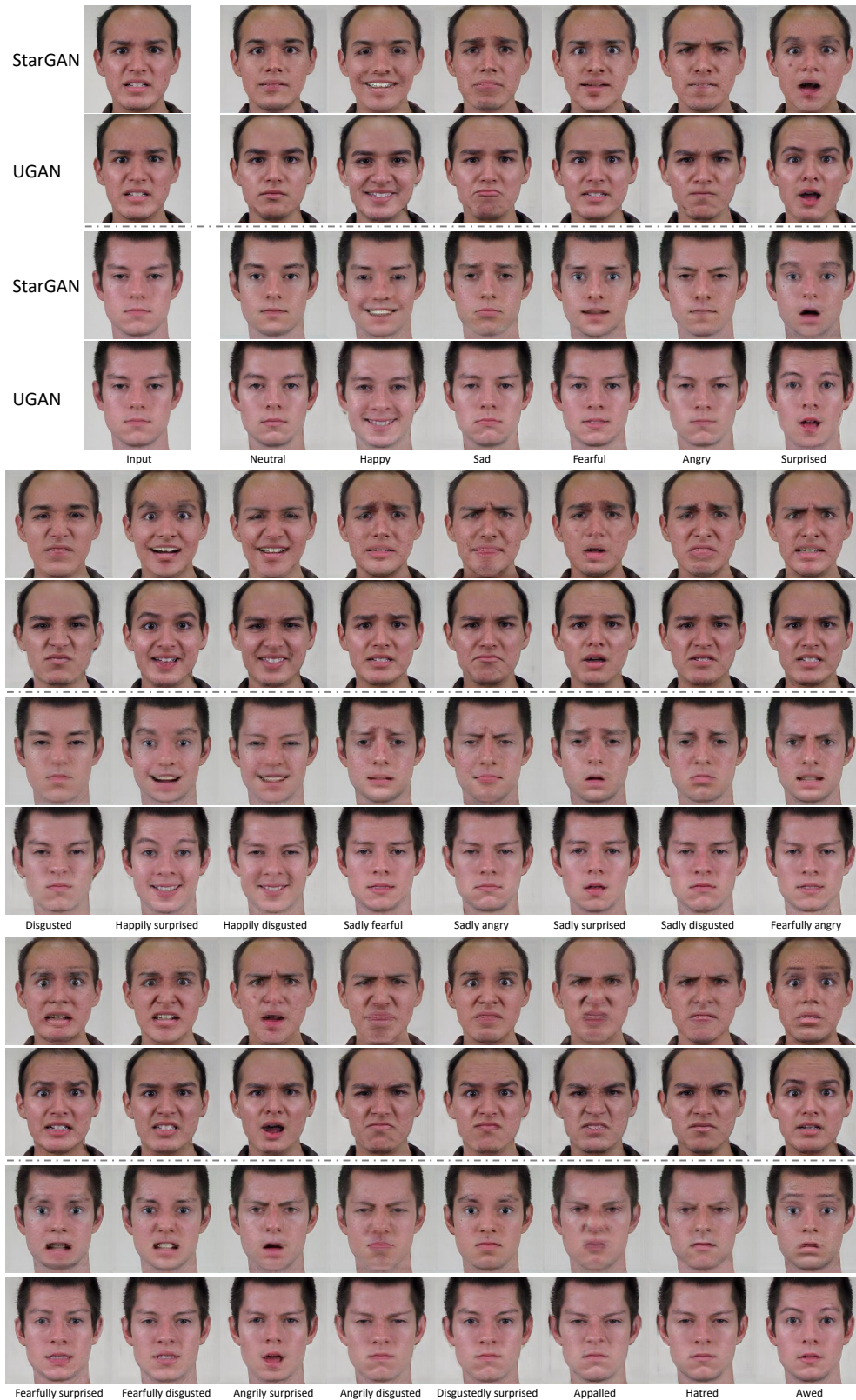


Figure 16. Expression editing results on the CFEE dataset.

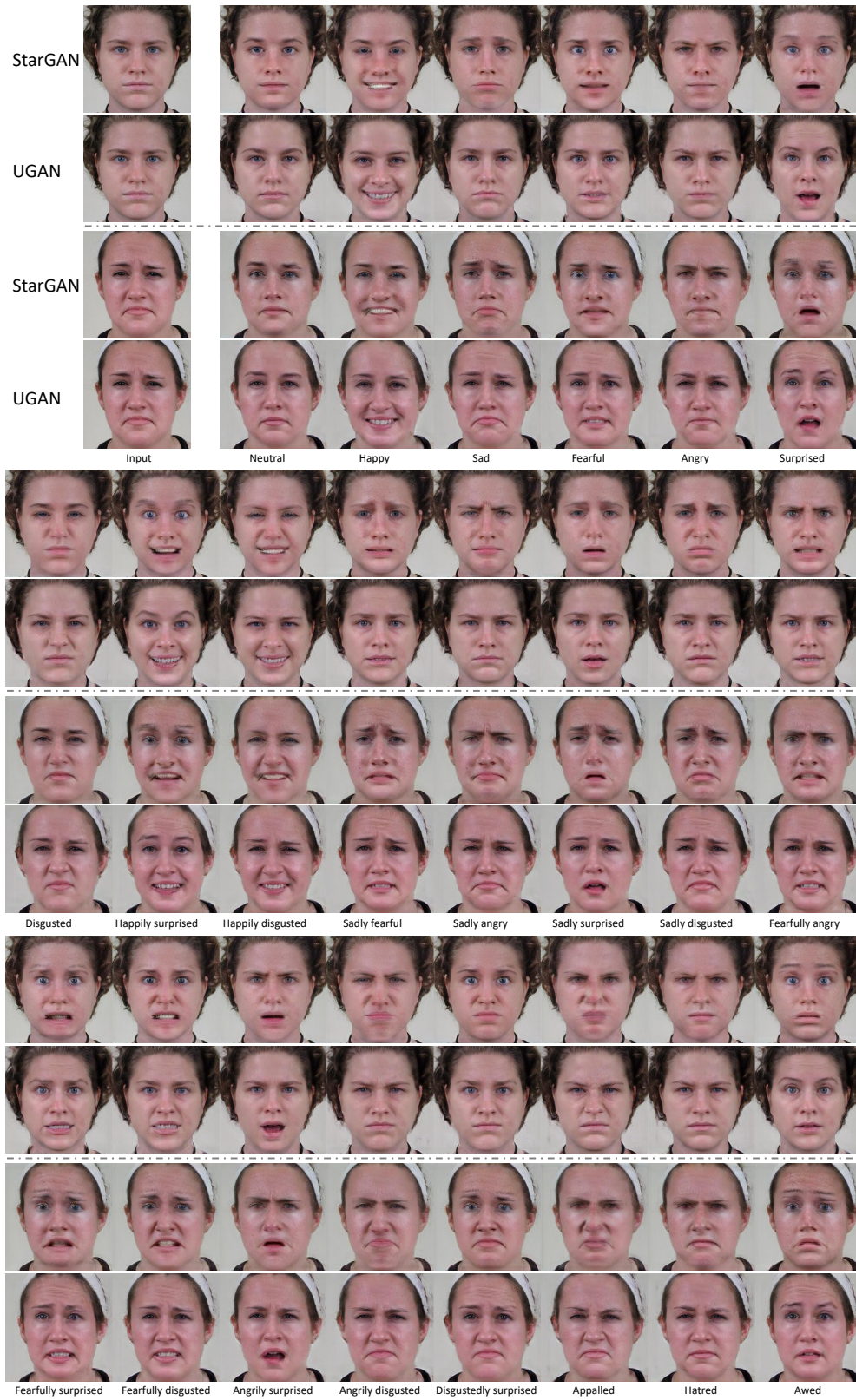


Figure 17. Expression editing results on the CFEE dataset.